Yellow: Sachs notes to himself and/or URAP mouse pod members or coauthors of this paper.

Synergy theory for murine Harderian gland tumors after irradiation by mixtures of high-energy ionized atomic nuclei

Edward Huang[1], Yimin Lin[1], Mark Ebert[1], Dae Woong Ham[3], Claire Yunzhi Zhang[1], Rainer K. Sachs[1,2]

[1] Department of Mathematics, University of California at Berkeley

[2] Corresponding Author, Rainer K. Sachs, sachs@math.berkeley.edu, 510-658-5790

[3] Department of Statistics, University of California at Berkeley

Abstract [212 words]

Murine Harderian gland (HG) tumorigenesis found in one-ion accelerator experiments with galactic cosmic ray (GCR) spectrum ions has been a NASA concern for many years. We describe synergy theory applicable to corresponding mixed-field experiments. The "obvious" approach of comparing an observed mixture dose-effect relationship (DER) to the sum of the components' DERs is known from other fields of biology to be unreliable when the components' DERs are highly curvilinear. Such curvilinearity may be present at low fluxes in the HG experiments due to non-targeted ('bystander') effects, in which case a replacement for simple effect additivity synergy theory is needed.

This paper studies a recently introduced, arguably optimal, replacement: incremental effect additivity (IEA). Customized open-source software is used. No new experimental results are presented. IEA is based on computer integration of non-linear ordinary differential equations. We discuss possible mixture experiments to illustrate IEA, including calculations of 95% confidence intervals. A web supplement discusses many peripheral issues. It includes arguments against NASA's emphasis on experiments with "representative" mixed beams most of whose dose is contributed by swift light ions.

Whether mixing GCR components sometimes leads to statistically significant synergy for tumorigenesis is not yet known. Significant synergy would increase risks for prolonged astronaut voyages in interplanetary space but hopefully does not occur.

1. Introduction

1.1. Scope of the paper

Murine Harderian gland (HG) tumorigenesis induced, in accelerator experiments, by ions in the galactic cosmic ray (GCR) spectrum has long been a NASA concern [Fry 1985, Curtis 1992, Alpen 1993, Alpen 1994, Chang 2016, Norbury 2016]. We here describe synergy theory applicable to corresponding mixed-field experiments.

The data considered consist of already published results. *In silico* calculations are tailored to analyze the first relevant experimental mixed beam results (which will become available soon), but are also used to discuss hypothetical mixed beams that illustrate some key points about synergy theory. Some of our analysis adapts to radiobiology ideas about synergy [reviewed, for example, in [Foucquier 2015]] developed in pharmacometrics, toxicology, evolutionary ecology and other fields.

Dose-effect relations (DERs) will play a central role. Typically the main information on mixed beam components comes from their individual one-ion DERs. The paper uses new DERs for the one-ion data. These are more parsimonious (i.e. have fewer adjustable parameters) than other recent models [Cucinotta 2013b, Chang 2016, Cucinotta 2017] for the same data. Because radiation biologists often have a strong preference for parsimony, the new models are of possible interest in their own right. However they are used in the present paper mainly because their relative simplicity facilitates synergy analysis of mixed radiation fields whose components have these one-ion IDERs.

Given one-ion DERs, synergy theory results can be calculated. The question to be answered is whether mixture data manifest synergy, antagonism, or neither. Importantly, synergy theory is applicable only to mixtures where the experimental conditions closely match the one-ion experiments that led to the one-ion IDERs [Berenbaum 1989, Ham 2018]. For example, the one-ion experiments considered in the present paper did not intentionally add shielding between upstream beam entry and the target, so we cannot usefully consider any mixtures which have shielding intentionally added. Similarly, almost all the one-ion experiments involved acute rather than protracted irradiation, so perforce we here will only consider mixtures where the total mixture dose is applied as rapidly as possible, typically within less than 10 minutes.

Synergy theory compares an experimentally observed mixture DER with a calculated baseline mixture DER defining the absence of synergy and absence of antagonism. Researchers in pharmacology and toxicology have known for a very long time [Fraser 1872, Loewe 1926] that the “obvious” method of comparing mixture effects with simply adding component effects is unreliable unless each mixture

component one-ion DER is approximately linear-no-threshold (LNT). This problem is reviewed, e.g., in [Zaider 1980, Berenbaum 1989, Geary 2013, Foucquier 2015, Piggott 2015, Tang 2015].

As a simple example of this unreliability, consider two agents with respective one-ion DERs $E_1 = \beta d_1^2$ and $E_2 = 2\beta d_2^2$, where β is a positive constant. These one-ion DERs, shown in Fig. 1, are curvilinear, since the second derivative (i.e. 2β or 4β respectively) is positive. Suppose we have a 50-50 mixture of the two agents, so that $d_1 = d/2$ and $d_2 = d/2$, where d is the total mixture dose. Then, since $(d/2)^2 = d^2/4$ the simple effect additivity (SEA) baseline no-synergy/antagonism effect, instead of being approximately the average of the two one-ion DER heights is only half that average. [when we submit the paper, figure numbering, equation numbering, and table numbering will be simplified; for the moment a messy system that facilitates later global search and replacement is being used].

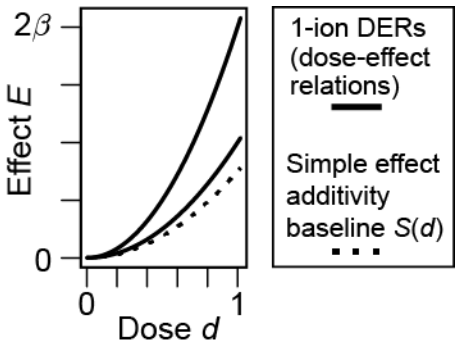

Fig. 1. SEA synergy theory often gives absurd criteria when component one-ion DERs are highly curvilinear. The dashed black line is the baseline no-synergy/antagonism mixture DER *S(d)* specified by the SEA theory for a 50-50 mixture of two agents. The two solid lines show the DERs that would result if one or the other mixture component supplied the total mixture dose *d* instead of just *d*/2. Any sensible synergy criterion would consider the dashed black curve, which specifies unexpectedly small mixture effects, as evidence for antagonism rather than using it as the baseline definition of neither synergy nor antagonism. Such discrepancies often arise when, as here, mixture component one-ion DERs are highly curvilinear. Consequently, many different replacements for SEA synergy theory are now in use to plan and interpret mixture experiments.

At sufficiently small radiation doses and high LETs, only a small fraction of all cell nuclei suffer a direct hit by a radiation track [Curtis 1992, Hanin 2014]. Non-targeted effects (NTE) are then sometimes important [Cucinotta 2010, Cucinotta 2013a, Hada 2014, Cacao 2016, Chang 2016, Cucinotta 2017, Shuryak 2017], with cells directly hit by an ion influencing nearby cells through intercellular signaling [Hatzi 2015]. The question of whether NTE are significantly carcinogenic at very low HZE doses remains open [Piotrowski 2017]. Models of NTE action that are smooth (i.e. have continuous derivatives of all orders) use one-ion DERs that are very curvilinear, with negative second derivative, at low doses [Brenner 2001]. So for small doses and high LETs replacements for the SEA synergy theory are needed to investigate mixtures whose component one-ion DERs take NTE into account.

The paper will use a replacement for SEA theory called incremental effect additivity (IEA). IEA theory was introduced in two recent papers [Siranart 2016, Ham 2017]. “Incremental” refers to the fact that one-ion DER slopes play an essential role in the theory. The underlying idea was suggested by G.K. Lam in 1987 [Lam 1987]. A one-ion DER slope defines a linear relation between a sufficiently small dose

increment and the corresponding effect increment; thus by analyzing sufficiently small increments one can circumvent the curvilinearities that plague SEA synergy theory. A systematic analysis of slopes requires using ordinary differential equations (ODEs) but Lam did not take this additional step. Implementing his insight has become practical because computers have become adept at integrating non-linear ODEs. An evaluation of his proposed replacement, called "independent action" [Lam 1994], for SEA is given in Online Resource 1, part 4. "Online Resource" refers to a .docx file we are allowed to place on the REBP Journal's web site. The file has to be called "ESM1". It acts as an appendix that can be very long without the expense of making a hard copy)

The two recent references [Siranart 2016, Ham 2017] that introduced IEA, after reviewing many other synergy theories, gave evidence that IEA synergy theory is probably the optimal substitute for SEA synergy theory. One important advantage of IEA synergy theory is that it obeys a "mixture of mixtures principle" [Ham 2017]; this principle is important because even nominally one-ion radiations are usually mixtures when they strike the HG, due to animal self-shielding or other matter in the beam. Another advantage [Ham 2017] is that the IEA theory can be applied to mixtures whose one-ion component DERs have very heterogeneous shapes.The present paper concentrates on explaining *in silico* IEA methodology.

A potential source of confusion for all synergy calculations is that three conceptually different kinds of DERs must be considered. The three kinds are: 1) individual one-ion DERs; 2) mixture baseline DERs that define absence of synergy and absence of antagonism; and 3), experimental mixture DERs, which may indicate synergy, or antagonism, or neither. Additional tricky points in the present paper are the following: 1) we will use different one-ion DERs for charge Z = 1 2 (in units of the proton charge) vs. charge $Z \geq 10$; and we will use only one-ion IDERs that assume both TE and NTE action, ignoring entirely alternative DERs that assume TE action only.

Because papers on synergy theory are sometimes over-optimistic as regards the usefulness of some specific synergy theory, we will also discuss drawbacks of IEA. For example, many (but not all) synergy theories do not even try to predict whether mixed-agent synergy will occur; they merely try to define what synergy is [reviewed in [Zaider 1980, Berenbaum 1989, Geary 2013, Kim 2015]]. Like SEA, IEA is among the synergy theories that have this drawback. Online Resource 1 (part 4) includes a systematic evaluation of IEA pros and cons.

1.2. Terminology

There will be a number of acronyms in this paper. Table 1.2.1 lists the main ones, with less familiar but here often used ones, such as DER and IEA, in bold-face and underlined. The table also lists some of our most frequently used mathematical symbols. Online Resource 1 (part 1)gives more detailed lists. ("Online Resource" refers to a .docx file we are allowed to place on the Journal's web site. The file has to be called "ESM1". It acts as an appendix that can be very long without the expense of making a hard copy)

Table 1.2.1. Main acronyms and mathematical notation used.

DER	dose-effect relation, for a single agent or a mixture; sometimes denoted by $E(d)$
$\mathbf{d}E/\mathbf{d}d$	A derivative. The slope of the one-ion DER $E(d)$
$D(E)$	compositional inverse function of a monotonic one-ion DER: $D(E(d)) = d$
$d_j = r_j d$	dose of the j^{th} mixture component as a fraction r_j of total mixture dose d
$E_j(d_j)$	one-ion DER for the j^{th} component of a mixture
$E(d)$	one-ion DER
$E(d; \boldsymbol{P})$	DER for an ion which is identified by its atomic charge, LET, and kinetic energy
GCR	galactic cosmic rays. The mixed radiation field in interplanetary space.
HG	Harderian gland. An organ found in many rodents
HZE	high Z (charge) and high energy atomic nuclei, almost fully ionized
IEA	incremental effect additivity. A synergy theory based on using ODEs
$I(d)$	IEA baseline no-synergy no-antagonism mixture DER
L=LET	linear energy transfer, stopping power, LET_∞
LNT	linear-no-threshold one-ion DER. A straight line with $E(0) = 0$
NTE	non-targeted effect(s) due to inter-cellular signaling. 'Bystander' effect(s)
ODE	ordinary differential equation
r_j	ratio of mixture component dose to total mixture dose, $r_j = d_j / d, 0 < r_j < 1$
SEA	simple effect additivity. The "obvious" but often inappropriate synergy theory.
$S(d)$	simple effect additivity baseline no-synergy/antagonism mixture DER
TE	targeted effect(s). Standard radiobiology action due to a direct hit or near miss
Y_0	background zero-dose HG prevalence for sham-irradiated controls
β^*	ion speed relative to the speed of light. $0 < \beta^* < 1$

1.3. Summary

The main purpose of this paper is to explain how IEA synergy theory can be applied to experiments on murine HG tumorigenesis induced by mixed radiation fields some of whose beamline-entering components are one-ion HZE beams. No new experimental data are presented.

The paper focusses on synergy theory techniques, emphasizing mathematical methods and customized computer programming more than biophysical insights. For example all our one-ion DERs for HZE ions will include terms that can model NTE in addition to terms for TE. Competing HZE one-ion DERs that assume TE-only action are here omitted because the one-ion DERs that model NTE in addition to TE can illustrate synergy theory techniques adequately. No implication that we consider joint-TE-NTE one-ion DERs for this data more plausible than TE-only one-ion DERs is intended.

Our approach to one-ion DERs for the data in [Fry 1985, Curtis 1992, Alpen 1993, Alpen 1994, Chang 2016] has been influenced by the work of Cucinotta and Chappell, including their seminal 2010 paper [Cucinotta 2010]. The papers foreshadow a number of our ideas, including the use of one-ion DERs highly curvillinear at very low dose for analyzing the murine HG data.

Recent one-ion DERs for the data [Cucinotta 2010, Cucinotta 2013b, Chang 2016, Cucinotta 2017] are based on modifications of Katz' amorphous track structure approach [Katz 1988, Cucinotta 1999, Goodhead 2006]. Our one-ion DERs in the present paper for the same data are, as discussed above, more parsimonious than the one-ion DERs based on the amorphous track structure approach. They achieve extra parsimony by taking full advantage of a hazard function equation, favored by Cucinotta and coworkers and reviewed in [Cucinotta 2017]. However the present paper, due to its emphasis on mathematical synergy theory rather than biophysical insights, does not attempt a balanced comparison of different one-ion DERs that would take into account goodness of fit as well as parsimony.

2. Methods

2.1. Customized Software

We use the open-source computer language R [Matloff 2011], initially designed for statistical calculations but now rapidly gaining acceptance among modelers [IEEE 2014]. Our customized programs are available at https://github.com/rainersachs/SynergyREBP/ and at Edward's repository. Readers can freely download, use and modify them to evaluate our conclusions critically.

2.2. one-ion DERs

A mixed radiation field consists of $N \geq 2$ components. Each component has a one-ion DER. Synergy theory starts with these one-ion DERs.

2.2.1. Standard one-ion DER properties

Fig. 2 illustrates "standard" properties that one-ion DERs considered in this paper will be assumed to have unless explicitly stated to the contrary; it also illustrates convexity/concavity terminology.

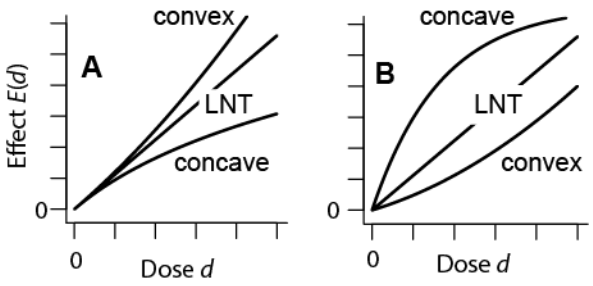

Fig. 2. one-ion DERs. Some relevant properties are here shown in a schematic graph that does not specify numerical values. The graph also serves to illustrate the terms "convex" and "concave". It is seen that convexity and concavity are characterized by the curvilinearity ("upwardly curving" or "downwardly curving"), not the curve location or slope.

"Standard" one-ion DER properties are the following.

1). For each mixture component when acting by itself, the data have background plus radiogenic contributions. We define the component's one-ion DER as the radiogenic contribution. Thus by definition one-ion DERs are zero when there is no dose above background. In Fig. 2 all curves start at the origin $d = 0$, $E = 0$

2). Standard one-ion DERs are continuous, continuously differentiable curves with a first derivative $\mathbf{d}E/\mathbf{d}d > 0$ for all non-negative doses d from zero up to the largest dose of interest. It follows that standard one-ion DERs are monotonic increasing for all doses of interest. Here "doses of interest" may be large. For example, even if an ion participating in a mixture contributes only half of the total mixture dose d and no experiments with $d > 1$ Gy are planned, the ion's one-ion DER is still

required to have positive first derivative all the way up to 1 Gy or in some cases even more, not just up to 0.5 Gy.

3). Standard one-ion DERs also have continuous second derivatives.

Non-standard one-ion DERs are often useful but are not needed for this paper. An example of a DER that violates properties 2) and 3) is a linear DER with threshold. At the threshold there is a kink where the first derivative is discontinuous and the second derivative is in effect a Dirac delta function so that, roughly speaking, it is $+\infty$ there.

As regards convexity and concavity: if the second derivative of a standard one-ion DER is respectively (positive, zero, or negative) for all doses of interest the one-ion DER is (strictly convex, LNT, or strictly concave) respectively, as shown in Fig 2.

Standard one-ion DERs can have shapes more complicated than those shown. Allowed, for example, are sigmoidal curves where the second derivative is positive at all small doses, is zero at one point of inflection, and is negative on up to the largest dose of interest [where, however, the slope is still required to be positive by property 2)].

2.2.2. Scope of the data

The data includes experimental observations on the fraction of female B6CF1/Anl mice that develop at least one radiogenic HG tumor after exposure at various doses to various one-ion GCR beams [Fry 1985, Curtis 1992, Alpen 1993, Alpen 1994, Chang 2016]. This fraction, the tumor prevalence, is by definition ≤ 1. As shown in Table 2.2.2.1, different ions differ in charge number Z, in LET L, in ion speed β^* relative to the speed of light, and in kinetic energy per atomic mass number KE/u. All data used in this paper is included in customized open-source software freely downloadable from GitHub.

Table 2.2.1. Ions Used.

ion	L	Z	β^*	KE/u	comments
	keV/μ			MeV	
^{1}H	0.4	1	0.614	250	Chang
^{4}He	1.6	2	0.595	228	Alpen
10Ne20	25	10	0.813	670	Alpen
14Si28	70	14	0.623	260	Chang
22Ti48	100	22	0.876	1000	Chang
26Fe56	193	26	0.793	600	Alpen
26Fe56	193	26	0.793	600	Chang
26Fe56	250	26	0.654	350	Alpen
43Nb93	464	43	0.793	600	Alpen
57La139	953	57	0.791	593	Alpen

In the Table 2.2.1, experiments done in the 20th century are labeled with Alpen; those done in the 21st century are labeled with Chang. Approximate LETs for the Alpen rows are for upstream beam entry; those for the Chang rows are at the surface of the animal. The row for 26Fe56 at 600 MeV/u labeled Chang is an exception where data from both centuries are combined, as described in detail in [Chang 2016]. There are two swift (β^* >0.5) light ($Z \leq 3$) ions, protons and alpha-particles, and 7 HZE ions, with ^{56}Fe at 600 Mev/u appearing in two different rows.

Sachs' reminder to himself. calculate_physics_data.R in minor sandbox files gives methods and results for calculating Katz' parameter and Z_{eff}. It should be included under minor files in GitHub for future reference for the big paper and the results should be included in ion characteristics in Online Resource 1 part 2.

Two of the physical parameters in Table 2.2.1 will be assembled into an ion-characterizing parameter vector with 2 components and used to label one-ion DERs as follows:

$$E(d; \boldsymbol{P}) \text{ where } \boldsymbol{P} = (Z, L). \qquad (2.2.3.1)$$

Sometimes $E(d; \boldsymbol{P})$ will be abbreviated as $E(d; L)$ since L in Table 2.2.1 uniquely determines Z; when there is no ambiguity, simply $E(d)$ will sometimes be used. Other recent models of the same data use a three-component physical parameter vector $\boldsymbol{P}$, with the third component being β^* or a parameter that, like a parameter used by Katz and coworkers, determines β^* when L and Z are given.

2.2.3. Omitted Data

Relevant experiments at the Brookhaven (NY) NASA space radiation laboratory (NSRL) are continuing. They involve additional one-ion beams or involve, for the first time, corresponding mixed-

beam exposures. The HG data from these ongoing experiments has not been published and will not be used in this paper. However, some of our synergy theory examples here were selected with ongoing or planning-stage mixed-beam experiments in mind.

2.2.4. HZE one-ion DERs: preliminary remarks

The one-ion DERs we use here for the HZE data modify some of the tumor prevalence models in [Chang 2016] and [Cucinotta 2017]. As mentioned in the Introduction section: (a) all relevant one-ion DERs, in the literature and in the present paper, assume TE dominate at high doses; (b) the HZE one-ion DERs we will use assume in addition that NTE dominate at low doses; and (c), this NTE assumption will not be critically evaluated. Recent modeling, e.g. [Chang 2016, Cucinotta 2017], considers NTE; one-ion DERs that assume NTE action in addition to TE action suffice to illustrate synergy theory methodology.

As a preview, Fig. 3 illustrates the shape of the HZE one-ion DERs that result from our assumption that NTE dominate at very low doses. The calculations, including regression, that lead to these shapes will be described only in subsequent sub-sections. The ion is ^{56}Fe with $Z = 26$, $L = 193$ keV/μm, and $KE = 600$ MeV/u.

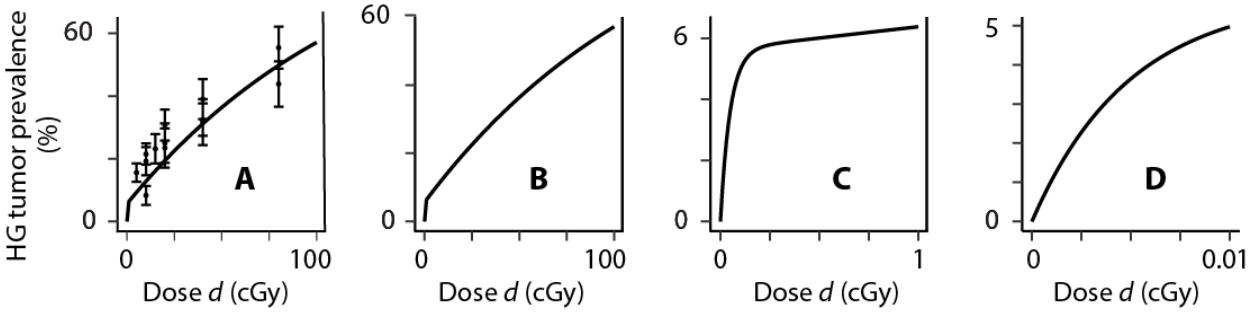

Fig. 3. HZE one-ion DER shapes. Panel A shows a DER obtained by regression. Panels B and C zoom in on panel A to give details on the very low dose region where NTE putatively dominate. ("Online Resource" refers to a .docx file we are allowed to place on the Journal's web site. The file has to be called "ESM1". It acts as an appendix that can be very long without the expense of making a hard copy).

Make crude range corrections for HE4 and Ne20 and Fe300 based on Fe 193 results ? Discuss this question in the online supplement

Our HZE one-ion DERs will be standard as defined in subsection 2.2.1. However, in panel A of Fig. 3 it looks as if standard smoothness conditions might be violated. The slope at $d = 0$ looks like it might be infinite; in addition it appears as if at one point there is a kink where the first derivate is discontinuous. Panel B zooms in to show that actually there is no kink, just a region of very high concavity. Panel C zooms in again to show that the slope at the origin is finite.

The overall shape (panel A) changes as dose increases. At very low doses there is very high concavity. Then there is a region where slight concavity and/or slight convexity can occur. Then at high

doses there must be concavity (despite the fact that in radiobiology high LET TE are often linear) due merely to the fact that prevalence, defined as presentation of at least one HG tumor, can never go above 100% no matter how large the dose.

Our HZE DER calculations will cover dose ranges larger than $0 \le d < 50$ cGy despite the fact that HZE doses of > 50 cGy are vigorously deprecated in some recent NASA calls. Some of the accumulated HG data we consider used higher doses, and there are two additional reasons. First, our modeling emphasizes the following idea. If an HZE ion is a component of a mixture, its relevant damage need not be the just the damage it itself would inflict if acting alone. More likely to be relevant is the incremental damage the ion inflicts when it adds its incremental dose to all the other incremental doses contributed by all the other mixture components. In this context, one-ion DER shapes at doses > 50 cGy remain relevant even if no high-dose experiments continue. The second reason is that we believe, and will in the Discussion section argue, that experiments with HZE doses considerably larger than those encountered even during several years above low earth orbit should be a major part of continuing efforts.

2.2.5. HZE one-ion DERs: the hazard function approach

The starting point for our models is a very useful hazard function equation [reviewed in [Cucinotta 2017]] suggested by Cucinotta and coworkers:

$$E(d) = 1 - \exp[-H(d)]. \qquad (2.2.5.1)$$

Here $E(d)$ is a one-ion DER and $H(d)$ is a non-negative hazard function, which can be chosen by biophysical modeling and then defines $E(d)$ via Eq. (2.2.5.1). Short calculations show that if $H(d)$ is chosen to be a standard DER (as defined above in connection with Fig. 2), then $E(d)$ in Eq. (2.2.5.1) is also a standard one-ion DER; for example, if $H(d)$ is chosen to have a positive first derivative then Eq. (2.2.5.1) implies that $E(d)$ has a positive first derivative, as required by the definition of a standard one-ion DER. We will use hazard functions which are standard DERs.

Eq. (2.2.5.1) is an important improvement over earlier models of the HG data. The equation implies that, no matter how large $H(d)$ becomes, $E(d) < 1$. Thus, without needing to add any extra adjustable parameters, Eq. (2.2.5.1) incorporates the limitation that $E(d) \le 1$, which must hold since prevalence is defined as having at least one HG tumor.

2.2.6. HZE one-ion DERs: the NTE term

Our HZE hazard functions will be taken to have additive NTE and TE contributions:

$$H(d; L) = N(d; L) + T(d; L). \qquad (2.2.6.1)$$

Here the NTE and TE contributions are denoted by N and T respectively.

We first consider the NTE contribution, N. This was taken to have the equation

$$N(d) = \eta\left[1 - \exp(-d / d_0\right]. \qquad (2.2.6.2)$$

In Eq. (2.2.6.2) η is an adjustable parameter, interpreted as the prevalence at which NTE for any HZE ion saturates so that, for prevalences larger than η, NTE, if any, are so small compared to TE that they are negligible (or are already included in TE models and in measured prevalences).

The other quantity, d_0, is a nominal dose chosen to be much smaller than 0.01 Gy; in our calculations we used 0.00001 Gy. There are no HZE data points in the region $0 < d < 0.033$ Gy. Data at higher doses do (perhaps) suggest NTE which lead to a large average positive slope, in the region $0 < d < 0.033$ Gy, whose cumulative influence builds up a prevalence large enough to be detectable above background and noise at doses ≥ 0.033 Gy.

To take into account NTE dose dependence in a way consistent with the concavity found in mechanistic models for NTE for other endpoints [Brenner 2001] we used the factor $[1-\exp(-d/d_0)]$ in Eq. (2.2.6.2) and used $d_0 = 10^{-5}$ Gy. Using Eq. (2.2.6.2) in NTE-TE models of our HG data is not new. Eq. (2.2.6.2), with a larger value of d_0, was used in [Cucinotta 2010], but inadvertently approximated as a discontinuous jump in that paper's text. Numerical explorations show that the final results of the present paper are insensitive to d_0 as long as $d_0 \ll 0.01$ Gy.

2.2.7. HZE one-ion DERs: TE term and newDERs

For the other term, T, in the HZE hazard equation (2.2.61) we devised new equations. After many attempts, we hit upon an algebraic combination of two adjustable parameters in earlier models that is, for the dose range of main interest, nearly dose-independent in those earlier models. Choosing this combination as one adjustable parameter allowed us to reduce the number of adjustable parameters from 4 to 3. "Parsimonious" models, with a minimal number of adjustable parameters in the spirit of Occam's razor, are often especially emphasized in radiobiology. Additional motives for using new models are detailed in Online Resource 1 (part 3)("Online Resource" refers to a .docx file we are allowed to place on the Journal's web site. The file has to be called "ESM1". It acts as an appendix that can be very long without the expense of making a hard copy).

Specifically, we used for H a TE term LNT in dose with a coefficient involving a standard two-parametric L dependence that typically peaks at an LET of several hundred keV/μm:

$$T(d;L) = a_1 L \exp\left(-a_2 L\right) d. \qquad (2.2.7.1)$$

Combining Eqs. (2.2.6.2) and (2.2.7.1) gives the comparatively simple equation for our new HZE model:

$$E(d;L) = 1 - \exp[-H(d;L)] \text{ where } H(d;L) = a_1 L \exp\left(-a_2 L\right) d + \eta\left[1 - \exp(-d / d_0\right]. \qquad (2.2.7.2)$$

The 3 adjustable parameters are a_1, a_2, and η.

2.2.8. HZE one-ion DERs: calibration methods and variance-covariance matrices

The background value, Y_0, for sham-irradiated controls was taken from [Chang 2016] to be $Y_0 = 2.7$ % prevalence, as estimated from all the zero-dose data, including older data not acquired at NSRL. In our paper here, Y_0 is regarded as an exact value. If one were attempting to compare a TE-only model with a

model that allows for both TE and NTE, the value of Y_0 and its variance would be very important (because at the very low doses where NTE putatively dominate TE, Y_0 and NTE have approximately the same magnitude). For reasons discussed above we did not consider TE-only models at all in this paper, where the emphasis is on synergy theory methodology rather than optimizing one-ion DERs, so taking Y_0 as fixed was adequate for our purposes here.

Given Y_0, the 3 adjustable parameters in the HZE one-ion DER of Eq. (2.2.7.2) were obtained by inverse-variance-weighted non-linear least squares regression. The variances were calculated by Ainsworth's formula $p(1-p)/n$ [Fry 1985], where p is prevalence and n is the number of animals at risk. The nls() function of the computer language R determined the variance-covariance matrix during the regression calculation, and this matrix was used in subsequent 95% confidence interval (CI) estimates for IEA baseline no-synergy/antagonism mixture DERs.

After calibration, our one-ion HZE DERs were considered applicable to all ions in the Z, LET, and kinetic energy ranges covered by the data, i.e. applicable even to one-ion beams not in the data set. The relevant Z and L ranges were given above: $10 \le Z \le 57$; approximate LET $25 \le L$ (keV/μm) ≤ 950. The kinetic energy range was $260 \le KE$/u (MeV) ≤ 1000.

2.2.9. One-ion DERs for low LET proton and alpha particle beams

The one-ion DER for data on $Z = 1$ or 2 ions was taken to be

$$E(d) = 1 - \exp[-H(d)] \quad \text{where} \quad H(d) = ad, \qquad (2.2.9.1)$$

where a is the only adjustable parameter, whose statistical distribution was determined by inverse-variance-weighted non-linear regression. We originally assumed a linear-quadratic form for the hazard function H, but the quadratic term was found to be not significantly different from zero so it was omitted from the model. As for HZE DERs, the hazard function approach thus facilitated use of parsimonious models.

When one-ion data for $2 < Z < 10$ is added to this HG data set, it would be reasonable to treat L as having a continuous spectrum. Like other one-ion DERs used, ours here in effect neglects the existence of biophysical similarities between the case $L \le 1.6$ keV/μm for $Z \le 2$ and the case $L \ge 25$ keV/μm for $Z \ge 10$.

2.3. Synergy theory calculations

2.3.1. Notation

Consider acute irradiation with a mixed beam of $N \geq 2$ different radiation qualities. The dose proportions r_j that the different qualities contribute to total dose $d = \sum_{j=1}^{N} d_j$ obey the equations

$$d_j = r_j d; \quad r_j > 0; \quad \sum_{j=1}^{N} r_j = 1. \qquad (2.3.1.1)$$

In our subsequent calculations r_j will always, for convenience, be independent of dose. Dose independent proportions r_j model one typical pattern for irradiation. The assumption of dose-independent proportions does not affect the final results. It implies that any one of the d_j can be considered a control variable on essentially the same footing as the total dose d since d_j determines d, via $d = d_j/r_j$ with $r_j > 0$, and thereby determines each $d_i = r_i d_j/r_j$. However we will distinguish sharply between the dose control variables d and d_j vs. total mixture effect considered as a control variable. In our analyses effect magnitude is sometimes used to determine d and d_j, instead of being determined by one of them.

2.3.2. SEA

Using the notations specified above, the baseline no-synergy/no-antagonism mixture DER of the SEA theory, denoted by $S(d)$, is:

$$S(d) = \sum_{j=1}^{N} E_j(d_j). \qquad (2.3.2.1)$$

2.3.3. Inverse functions

Inverse functions (sometimes called compositional inverse functions) play a prominent role in various synergy theories, including IEA. Inverse functions are needed when using effect, rather than dose, as the independent variable. A familiar radiobiology example of inverse functions occurs when calculating the relative biological effectiveness (RBE) of two different radiations.

The inverse of a monotonically increasing function undoes the action of the function. For example, for x > 0, $\sqrt{x^2} = x$ so the positive square root function is the inverse of the squaring function; note that the inverse of x^2 is not x^{-2}. As another example $\exp[\ln(x)] = x$ for $x > 0$, and $\ln[\exp(y)] = y$ so the functions exp and ln are inverses of each other.

2.3.4. The IEA equation that defines absence of synergy and absence of antagonism

When the SEA synergy theory is inappropriate, an IEA baseline no-synergy/antagonism mixture DER $I(d)$ has a number of conceptual and practical advantages over other known replacements for $S(d)$. [Siranart 2016]. This subsection defines the elementary version of $I(d)$, which suffices for the present paper; there is a much more general version [Ham 2017] that we do not need here.

Suppose we have a mixture of N components with each component one-ion DER 'standard' as defined when discussing Fig. 2. It follows that each component one-ion DER has a compositional inverse function D_j, defined for all doses of interest and thus for all sufficiently small non-negative effects E. As discussed in sub-section 2.3.3 this means $D_j(E) = d$ when $E = E(d)$. The baseline IEA no-synergy no-antagonism mixture DER $I(d)$ is defined as the solution of the following initial value problem for a first order, typically non-linear, ODE:

$$\mathbf{d}I / \mathbf{d}d = \sum_{j=1}^{N} r_j \left[\mathbf{d}E_j / \mathbf{d}d_j \right]_{d_j = D_j(I)}; \; d = 0 \Leftrightarrow I = 0, \qquad (2.3.4.1)$$

with r_j = constant > 0 being again the fraction of the total mixture dose contributed by the j^{th} component. Thus the k^{th} one-ion DER also obeys Eq. (2.3.4.1) but with $r_k = 1$ and all the other $r_j = 0$. Under our assumptions there is a unique, monotonically increasing solution $I(d)$ for all doses of interest [Ham 2017].

In Eq. (2.3.4.1), the square bracket with its subscript indicates the following calculations. First find the slope of the j^{th} one-ion DER curve as a function of individual dose d_j. Then evaluate d_j using the inverse function D_j with the argument of D_j being the effect I already present due to the influence of all the components acting jointly. Using $d_j = D_j(I)$ in Eq. (3) instead of the seemingly more natural $d_j = D_j(E_j)$ is the key assumption made. Using $d_j = D_j(E_j)$ would merely lead back to the SEA baseline mixture DER $S(d)$ [Ham 2017].

Eq. (2.3.4.1) can be interpreted as follows. As the total mixture dose d increases slightly, every individual component dose d_j has a slight proportional increase since $\mathbf{d}d_j / \mathbf{d}d = r_j > 0$. Therefore every mixture component contributes some incremental effect. The size of the incremental effect is determined by the state of the biological target, specifically by the total effect already contributed by all the components collectively (and <u>not</u> by the dose the individual component has already contributed). In this way different components appropriately track changes of slope both in their own one-ion DER and in the other one-ion DERs.

2.3.5. Calibrating Background and Radiogenic Effects Separately

Synergy is typically considered as due to interactions among agents. Our mathematical synergy analysis applies to radiogenic effects. In calibrating one-ion DERs $E_j(d_j)$ from data we always, as discussed above, used only data at non-zero doses, $E_j(0)$ being 0 by definition. Background, designated by Y_0, was based on the zero-dose data for sham irradiated controls. Y_0 is needed when calibrating one-ion DERs from data or comparing baseline mixture DERs to data. However the main synergy calculations involve only one-ion DERs, not background plus radiogenic, effects.

2.4. Uncertainties in mixture effects

Synergy theory requires not only a way to calculate a baseline mixture DER defining no-synergy/no-antagonism but also a method of estimating uncertainties for the baseline mixture DER from mixture component one-ion DER uncertainties. Taken together these two elements constitute a default hypothesis useful for statistical significance tests on mixture observations. Without such tests, it is sometimes unclear if an unexpectedly large or small observed result does or doesn't call for a follow-up experiment. We used Monte Carlo simulations [Binder 1995] to calculate 95% CI for $I(d)$. Because it is known that neglecting correlations between calibrated parameters tends to overestimate how large CI are [Hanin 2002, Ham 2017], we took such correlations into account using variance-covariance matrices and matched correlation matrices.

2.5. Summary of *in-silico* synergy theory methodology

Fig. 4 summarizes our synergy calculations in a flow chart that with minor rewording would also apply to many other synergy theory papers. The flow chart re-emphasizes that three conceptually different kinds of DERs are involved.

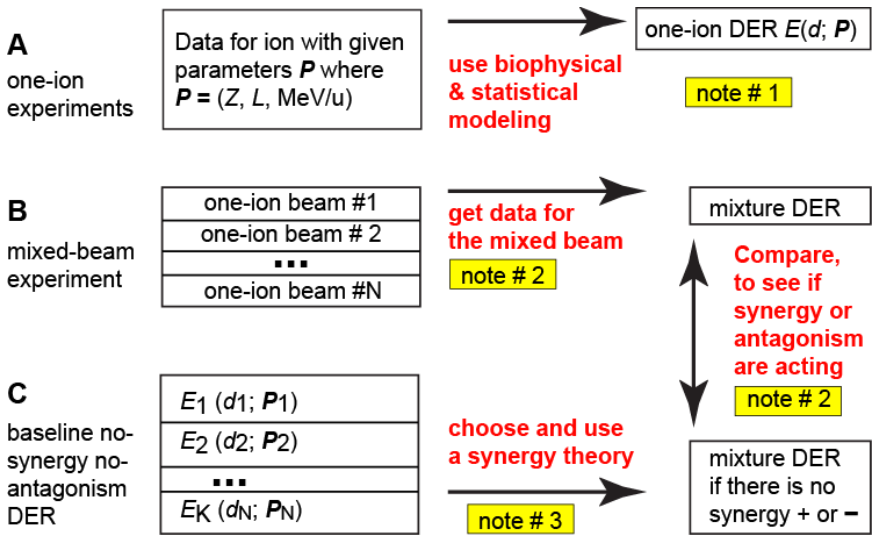

Fig. 4. Synergy modeling. Notes explaining some details are given in the text.

Note # 1. In our hands the biophysical and statistical modeling of one-ion DERs is not systematic. It uses educated guesswork trying to assemble many different kinds of biophysical, mathematical, and statistical information into equations.

Note # 2 (applies to both spots where it is shown on Fig. 4). No published results on mixed beams are yet available in this data set. We will here discuss instead mixed beams for which data will soon be available, mixed beams tentatively planned, mixed beam experiments we believe should be carried out

but most probably will not be carried out, and purely hypothetical mixed beams discussed only because they illustrate some aspect of synergy theory.

Note # 3. For brevity, SEA and IEA are the only synergy theories for which this paper gives any graphs, tables, or numerical results.

Online Resource 1 (part 5) gives a detailed description of the freely downloadable open-source R script that implements the methods shown in Fig. 4.

2.6. Combinatorial complexity

The approach shown in Fig. 4 confirmed a surprising major problem first described in [Ham 2017]: investigating synergy for multi-ion beams systematically is flatly impossible because there are too many possible mixtures that would need to be considered. For example suppose a 50-50 mixture of 2 ions does not show synergy. A systematic approach would presumably call for 2 further experiments, one with, say, a 85%-15% mixture of the same two radiation qualities, the other a 15%-85% mixture – a total of three experiments instead of just one. The startling aspect is that if one starts with, say, a seven-ion mixture where each ion contributes 1/7 of the dose and applies the same line of reasoning one sees that a systematic approach would presumably require millions of experiments rather than just one: combinatorial complexity for possible dose fractions leads to an extraordinarily rapid increase as the number of mixture components increases.

3. Results

3.1. One-ion DERs

3.1.1. Low LET results needs corrections for NWeight revision 4/1/2018, as do all other results

The DER for swift light ions, Eq. (2.2.9.1), contains one adjustable parameter, α. Calibrating α by regression gave $\alpha = 0.15204 \pm 0.01239$, where 0.01239 is the standard error of the mean; thus, for example, the estimated probability that α is larger than 0.15204 + (1.96 times 0.01239) is about 2.5%. Fig. 5 shows the DER, the non-zero-dose data points for protons and α-particles, and the 95% empirical CI for each data point.

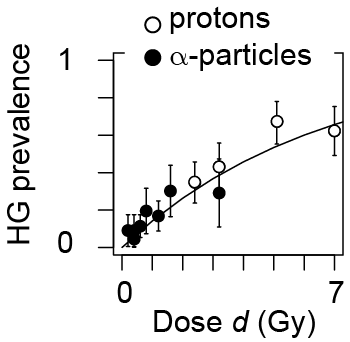

Fig. 5. Low LET data and models. In this paper all one-ion beams for Z ≤ 2 are modeled by the same one-ion DER, shown as the curve in the figure. Also shown are all the data points with their empirical error bars; for example the tops of the error bars are 1.96 standard deviations above the data points, so, assuming Gaussian distributions, the total error bar height intervals correspond to 95% CI.

Since our emphasis in this paper is more on synergy theory than on devising biophysically optimal one-ion DERs. The parsimonious one-parameter fit shown in Fig. 5 is adequate for our purposes.

3.1.2. High LET results

The one-ion DERs emphasized in this paper are for high LET ions. Calibration results, for the 3 adjustable parameters of our HZE DERs given in Eq. (2.2.9.1), are shown in Table 3.1.2.1.

Table 3.1.2.1. Statistics for HZE model. Here "e" refers to powers of 10, e.g. 2.17e-07 = 2.17 times 10^{-7}. It is seen that all 3 adjustable parameters differ significantly from 0, indicating parsimony.

Parameter	Estimate	SE	t value	Pr(>|t|)	level
a_1 (μ keV^{-1} Gy^{-1})	0.6798	0.107	6.341	2.17e-07	$p << 0.001$
a_2 (μ keV^{-1})	3.198e-3	5.36e-4	5.97	6.94e-07	$p << 0.001$
η (%)	6.267	1.136	5.51	2.86e-06	$p << 0.001$

The resulting HZE DERs and all the data used in this paper are shown in an 8-panel figure in Online Resource 1 (part 3); they are also contained in the scripts freely downloadable from GitHub. "Online Resource" refers to a .docx file we are allowed to place on the Journal's web site. The file has to be called "ESM1". It acts as an appendix that can be very long without the expense of making a hard copy.

For later analyses of IEA baseline mixture DER CI, we recorded parameter variance-covariance and correlation matrices for our HZE DERs, with the results shown in Table 3.1.2.2.

Table 3.1.2.2. Adjustable parameter variance-covariance matrix and correlation matrix.

Here "e" refers to powers of 10, e.g. 1.149e-02 = 0.001149.

	variance-covariance matrix			correlations		
parameter	a_1	a_2	η	a_1	a_2	η
a_1 (μ keV^{-1} Gy^{-1})	1.149e-02	4.5072e-05	-5.313e-02	1	0.78	-0.44
a_2 (μ keV^{-1})	4.507e-05	2.872e-07	-4.843e-05	0.78	1	-0.08
η (%)	-5.313e-02	-4.843e-05	1.2915	-0.44	-0.08	1

3.2. Mixture baseline no-synergy/antagonism DERs

The preceding subsection describes our results for one-ion DERs of our synergy modeling flow chart, Fig. 4 row A. No relevant published information on murine HG mixture experiments (row B of the flow chart) is yet available. Thus we now turn to illustrating our main results, corresponding to row C of the flow chart. This subsection illustrates the IEA no-synergy/antagonism baseline $I(d)$ with examples and compares it with the SEA synergy theory baseline $S(d)$ that $I(d)$ is designed to replace. Examples of 95% CI for $I(d)$ are postponed till later. As explained in the Introduction, all mixtures described in this subsection of the Results section (and in all other subsections of the Results section) are perforce considered to involve acute irradiation and to have no extra shielding intentionally added.

Fig. 6 shows, as an example, results for a 2-ion mixture. A recent NSRL irradiation whose outcome has not yet been scored used (in different proportions) the same 2 ions, the low LET component being protons with KE = 250 MeV/u.

Fig. 6. Mixtures of one HZE and one low LET ion. Both panels show effects due to a total mixture dose d. For illustrative purposes the maximum d value 3 Gy shown is larger than values which we will use in later figures.

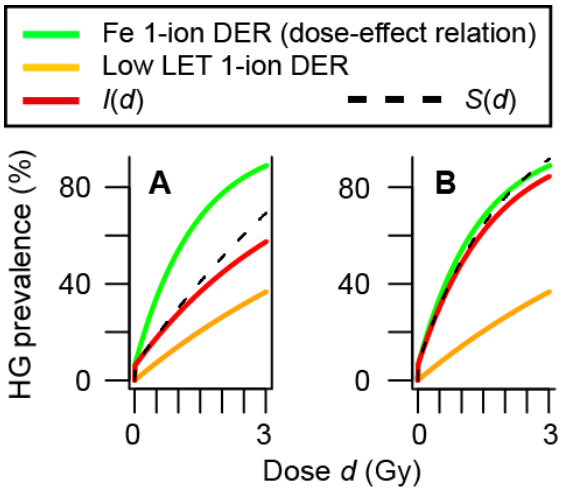

In panel A. swift light ions contribute 80% of the total mixture dose and an HZE beam of Fe56 ions with KE= 600 MeV/u and charge Z of almost 26 proton charges contributes the remaining 20%. In panel B the two proportions are reversed, with swift light ions contributing only 20% of the total mixture dose d.

In both panels the green and orange curves show the effect that would result if the corresponding one-ion beam contributed the entire mixture dose instead of only a proportion; thus these curves are exactly the same in both panels. Comparing panels A and B, both the red and black baseline mixture DER curves are lower in panel A, as one would expect from the fact that the low LET beam, which has the lower one-ion DER, contributes 80% of the dose in panel A but only 20% in panel B.

The red curve, defining incremental effect additivity synergy theory's baseline no-synergy antagonism DER, here always lies between the two one-ion DERs and thus below the green Fe curve, as one would expect from the qualitative idea that effects bigger than those estimated from analyzing one-ion DERs should be taken as indicating synergy rather than defining absence of synergy. However, it

is seen that near total mixture dose 3 Gy the SEA theory's definition of no synergy is actually a little higher than the green curve.

In actual experiments one usually aims for a maximum HG prevalence of around 25%-35%, not the larger effects determined by $S(d)$ or $I(d)$ for doses above about 1 Gy in Fig. 6. A prevalence of 25-35% is typically large enough to give a positive control for value and for trend without mouse mortality becoming a major confounding factor. The maximum dose of 3 Gy in Fig. 6 is larger than doses typically used in the one-ion accelerator experiments. Possible drastic solar particle events apart, it is much larger than any that would be expected even in a prolonged interplanetary voyage.

The formalism can handle almost any number of HZE ions. Fig. 7 gives an illustrative example somewhat similar to an upcoming experiment. The 20% HZE fraction of the total mixture dose in panel A of Fig. 6 is redistributed to 4 HZE ions of respective LETs 40, 110, 180, and 250 keV/μ. As in Fig. 6, 80% of the total dose is contributed by any mixture of swift $Z \leq 3$ ions, all these low LET contributions being modeled by the same one-ion DER.

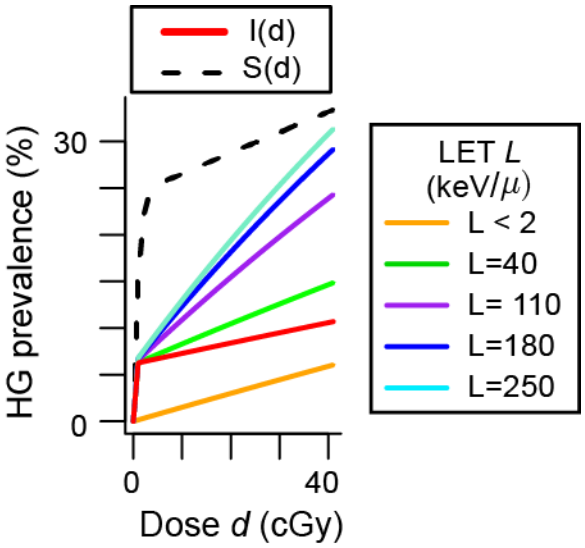

Fig. 7. A five-ion mixture. The low LET radiation contributes 80% of the total mixture dose d and each of the four HZE ions contributes 5%. As in Fig. 6. the DERs that each radiation quality would have if it contributed the entire mixture dose are shown in addition to the IEA baseline $I(d)$ and SEA baseline $S(d)$. It is not obvious from the figure but each one-ion DER is twice continuously differentiable, has negative second derivative at all doses of interest, and is thus strictly concave. For example the apparent kink in each HZE DER at prevalence of about 6% is actually a region of extremely high concavity. It is seen that $I(d)$ is between the 5 one-ion DERs but $S(d)$ is higher than any of the 5.

In Fig. 7, the red baseline IEA curve $I(d)$ is a reasonable definition of no-synergy/antagonism for the mixture, intermediate between the various component DERs. Intuitively speaking, it is here below all the HZE DERs because so much of the total dose is contributed by low LET radiation (orange curve). SEA theory, however, makes the absurd claim that some mixture effects larger than any component radiation could produce on its own are not evidence for synergy but rather define absence of synergy. This inability of SEA to handle the curvilinearities shown is typical. As reviewed in Online Resource 1 (part 4), $S(d)$ is always an unrealistic over-estimate when all components of a mixture have concave DERs.

Synergy theory results for an experiment whose results will hopefully soon be available are shown in Fig. 8. Both mixture components are HZE, with the very high RBE for murine HG tumorigenesis, perhaps about 40 or more, that has long been a major concern as regards sending astronauts on prolonged missions above low earth orbit. The experiment may give indications of whether or not there is synergy between HZE components that would make a mixture even more dangerous than the high component RBEs would suggest. This may be the only murine HG tumor experiment that will ever be performed at NSRL which is suitable for this purpose. At present NASA insists that a large majority of the dose on entering the beam in upcoming murine HG mixed field experiments be in swift light ions. The comparatively well understood swift light ions produce effects that severely confound analyses of possible HZE-HZE synergy.

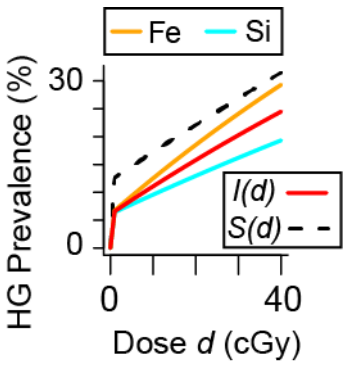

Fig. 8. A 50-50 mixture of two HZE components. The orange and blue curves show DERs, based on previous one-ion experiments, for the effects either ion would produce if it carried all the mixture dose *d* instead of only half. The red and dashed black curves show baseline no-synergy/antagonism mixture DERs: *I*(*d*) for the IEA synergy theory and *S*(*d*) for the SEA theory. It is seen that *S*(*d*) is, as in Fig. 7, unacceptably high. As reviewed in Online Resource 1 (part 4), *S*(*d*) is always an unrealistic over-estimate when, as in this mixture, all components have concave DERs.

There are many further examples which illustrate various aspects of IEA synergy theory – far too many to study systematically even *in vitro*, as explained in the Methods subsection on combinatorial complexity. Our final example here, Fig. 9, is a hypothetical mixture of all seven HZE ions in Table 2.2.1, each contributing 1/7 of the total mixture dose *d*.

Explain why some lines are dashed. Correct with Claire .csv data. The higher LET Fe56 is not 300 but rather 350 Mev/u. Don't ever use yellow for lines, yellow is excellent for background but invisible for lines.

Fig. 9. A mixture of 7 HZE ions.

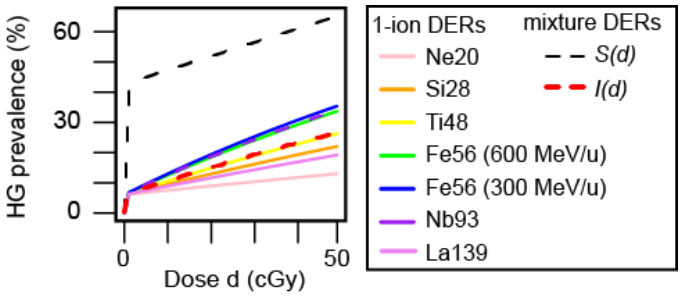

3.3. Mixture CI

Fig. 3.3.1. Ribbon plot for IEA in Fig. 7; omit simple effect additivity entirely from here on

Fig. 3.3.2. Ribbon plot for Fig 8: two panels, comparing correct ribbon with ribbon that neglects correlations. panels lined up horizontally so that one can see the difference. add hypothetical point that shows statistically significant synergy which seems to be not significant at the 95% CI level in the incorrect plot. Here is a CA plot which shows the basic idea

Template for Fig. 3.3.2

Data published by Hada and coworkers, 2014 and 2016: six 1-ion HZE beams, with 75 keV/μm ≤ L ≤ 240 keV/μm and 8 ≤ Z ≤ 26. Some of their models, & our models shown, included both TE and NTE.

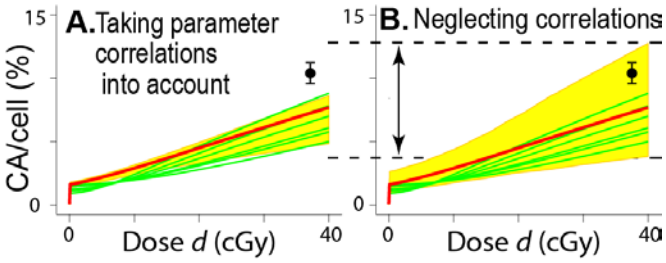

4. Discussion

4.1 Comments on the results

To illustrate IEA synergy theory we gave results exemplifying the following: the importance of having high-quality one-ion DERs available; the use of IEA as an alternative to SEA when one-ion DER curvilinearity requires an alternative; calculation of baseline mixture DER 95% CI

taking into account correlations between one-ion DER adjustable parameters so that much tighter CI are properly identified; and the extraordinarily rapid increase in the number of possible mixtures needed to determine synergy patterns for N-component mixtures as N increases. We criticized NASA's current emphasis on experiments with "representative" mixed beams in which the majority of the dose is contributed by swift light ions; Online Resources 1 (part 4.3) gives a long list of reasons why we consider this emphasis inappropriate for murine HG and other experiments.

The quality of the fit of our one-ion DERs (indicated by Fig. 5 and Table 3.2.1.1) was considered adequate for illustrating mixture DER behavior so we did not investigate whether alternative one-ion DERs rrr based on TE-only or amorphous track structure approaches might be superior.

In Fig. 8. The absurdly large values of $S(d)$ at very small doses violate not only intuitive ideas of what synergy means but also biophysical reasoning. Such large values correspond to the picture that during acute irradiation low-dose NTE effects in a mixture saturate at the sum of the components' NTE. But biophysical reasoning would suggest for acute doses something like the average instead of the sum. Consider two radiation qualities, say A and B. One-ion experiments strongly suggest that once radiation quality A causes cell #1 in a multi-cell interaction region corresponding to the NTE signal range to send out a NTE signal saturation occurs: a second hit on cell #2 in the same interaction region by radiation A causing cell #2 to send out additional bystander signals does not further enhance NTE noticeably. To suppose that if it is instead radiation quality B that hits cell #2, causes a bystander signal that would be almost ignored if the hit were by quality A, and thereby doubles NTE is far-fetched. How are the bystander cells, bombarded by a mixture of radiation qualities A and B, supposed to know the radiation quality of the radiation that affected cell # 2? Thus Fig. 8 merely illustrates, once again, that relying on SEA synergy theory can be very misleading – a fact that has too often been ignored during the last 150 years.

4.2 Synergy theory in radiobiology

For the foreseeable future radiobiologists studying mixed radiation field effects will almost inevitably emphasize possible synergy and antagonism among the different radiation qualities in the mixture. Therefore trying to find a systematic quantification of synergy, general enough to cover most cases of radiobiological interest and precise enough to enable credible estimates of statistical significance when synergy is indicated by a mixture experiment, is worthwhile. But it is not easy.

One main problem is the following. The common belief that synergy can always be defined as an effect greater than the SEA baseline mixture DER $S(d)$ is wrong. In some important cases $S(d)$ is clearly inappropriate. There are a number of published alternatives which seem appropriate whenever they can be calculated, but are not well defined unless all one-ion DERs in a mixture are monotonic in the same direction. This monotonicity requirement restricts their scope unduly.

Among the alternatives to $S(d)$, the IEA baseline mixture DER $I(d)$ seems preferable. We have here illustrated it with detailed examples of mixtures of ions in the GCR spectrum, since more experimental information on such mixtures will soon become available. All known synergy theories, including IEA, have substantial limitations. Online Resources 1 (part 4.xxx) lists many of these.

4.3. Summary

- Synergy theory will continue to be used to plan experiments involving mixed radiation fields and interpret the results of such experiments. It can and should include calculations that give 95% confidence intervals based on variance-covariance matrices.
- If non-targeted effects are important the SEA no-synergy/no-antagonism baseline mixture DERs should be ignored or used only cautiously.
- IEA theory is in our opinion the optimal choice when a replacement for SEA synergy theory is needed.
- When individual dose-effect relations for components of a mixture are all monotonically increasing there are many other synergy theories that have been developed over many years in many different fields of biology to supplement or replace SEA.
- In any case, all synergy theories have more limitations than is generally realized.
- Whether mixing GCR components ever leads to statistically significant synergy for animal tumorigenesis is not clear. Upcoming mixture experiments will hopefully help clarify this question.

Acknowledgements:

RKS is grateful for support from NASA grant NNJ16HP22*1*. DWH, EH, ME, JY, YL, and CYZ are grateful for support from the UC Berkeley undergraduate research apprenticeship program (URAP). We are grateful to Dr. E.A. Blakely, Dr. P.Y. Chang, Dr. M. Hada, Dr. L. Chappell, and Dr. J.H. Mao for useful discussions. We thank Dr. F.A. Cucinotta, Dr. M. Hada, and Dr. L. Chappell for clarifying some details of the data sets.

Bibliography

1. Alpen, EL, et al. (1993). "Tumorigenic potential of high-Z, high-LET charged-particle radiations." Radiat Res **136**(3): 382-391.

2. Alpen, EL, et al. (1994). "Fluence-based relative biological effectiveness for charged particle carcinogenesis in mouse Harderian gland." Adv Space Res **14**(10): 573-581.
3. Berenbaum, MC (1989). "What is synergy?" Pharmacol Rev **41**(2): 93-141.
4. Binder, K (1995). Introduction: General Aspects of Computer Simulation Techniques and Their Applications in Polymer Physics. Monte Carlo and Molecular Dynamics Simulations in Polymer Science. K. Binder. Oxford, Oxford University Press.
5. Brenner, DJ, et al. (2001). "The bystander effect in radiation oncogenesis: II. A quantitative model." Radiation Research **155**(3): 402-408.
6. Cacao, E, et al. (2016). "Relative Biological Effectiveness of HZE Particles for Chromosomal Exchanges and Other Surrogate Cancer Risk Endpoints." PLoS One **11**(4): e0153998.
7. Chang, PY, et al. (2016). "Harderian Gland Tumorigenesis: Low-Dose and LET Response." Radiat Res **185**(5): 449-460.
8. Cucinotta, FA, et al. (2017). "Non-Targeted Effects Models Predict Significantly Higher Mars Mission Cancer Risk than Targeted Effects Models." Sci Rep **7**(1): 1832.
9. Cucinotta, FA, et al. (2010). "Non-targeted effects and the dose response for heavy ion tumor induction." Mutat Res **687**(1-2): 49-53.
10. Cucinotta, FA, et al. (2013a). Space Radiation Cancer Risk Projections and Uncertainties – 2012. Hanover, MD; http://ston.jsc.nasa.gov/collections/TRS, NASA Center for AeroSpace Information.
11. Cucinotta, FA, et al. (2013b). "How safe is safe enough? Radiation risk for a human mission to Mars." PLoS One **8**(10): e74988.
12. Cucinotta, FA, et al. (1999). "Applications of amorphous track models in radiation biology." Radiat Environ Biophys **38**(2): 81-92.
13. Curtis, SB, et al. (1992). "Fluence-related risk coefficients using the Harderian gland data as an example." Adv Space Res **12**(2-3): 407-416.
14. Foucquier, J, et al. (2015). "Analysis of drug combinations: current methodological landscape." Pharmacol Res Perspect **3**(3): e00149.
15. Fraser, TR (1872). "Lecture on the Antagonism between the Actions of Active Substances." Br Med J **2**(618): 485-487.
16. Fry, RJ, et al. (1985). "High-LET radiation carcinogenesis." Radiat Res Suppl **8**: S188-195.
17. Geary, N (2013). "Understanding synergy." Am J Physiol Endocrinol Metab **304**(3): E237-253.
18. Goodhead, DT (2006). "Energy deposition stochastics and track structure: what about the target?" Radiat Prot Dosimetry **122**(1-4): 3-15.
19. Hada, M, et al. (2014). "Induction of chromosomal aberrations at fluences of less than one HZE particle per cell nucleus." Radiat Res **182**(4): 368-379.
20. Ham, DW, et al. (2017). "Synergy Theory in Radiobiology." Radiat Res.
21. Ham, DW, et al. (2018). "Synergy Theory in Radiobiology." Radiat Res **189**(3): 225-237.
22. Hanin, L (2002). "Identification Problem for Stochastic Models with Application to Carcinogenesis, Cancer Detection and Radiation Biology." Discrete Dynamics in Nature and Society **7**(3): 177-189.
23. Hanin, L, et al. (2014). "On the probability of cure for heavy-ion radiotherapy." Phys Med Biol **59**(14): 3829-3842.
24. Hatzi, VI, et al. (2015). "Non-targeted radiation effects in vivo: a critical glance of the future in radiobiology." Cancer Lett **356**(1): 34-42.

25. IEEE. (2014). "Inst. Electric and Electronic Engineers: Top 10 Programming Languages." Retrieved 03/2015, from http://spectrum.ieee.org/computing/software/top-10-programming-languages.
26. Katz, R. (1988). "Radiobiological Modeling Based On Track Structure. Quantitative Mathematical Models in Radiation Biology, ed. J. Kiefer." Retrieved December, 2016, from http://digitalcommons.unl.edu/physicskatz/60.
27. Kim, MH, et al. (2015). "Issues for Simulation of Galactic Cosmic Ray Exposures for Radiobiological Research at Ground-Based Accelerators." Front Oncol **5**: 122.
28. Lam, GK (1987). "The interaction of radiations of different LET." Phys Med Biol **32**(10): 1291-1309.
29. Lam, GK (1994). "A general formulation of the concept of independent action for the combined effects of agents." Bull Math Biol **56**(5): 959-980.
30. Loewe, S, et al. (1926). "Ueber Kombinationswirkungen. I. Mitteilung Hilfsmittel der Fragestellung." Archiv for Experimentelle Pathologie und Pharmakologie **114**: 313-326.
31. Matloff, N (2011). The Art of R Programming. San Francisco, No Starch Press.
32. Norbury, JW, et al. (2016). "Galactic cosmic ray simulation at the NASA Space Radiation Laboratory." Life Sci Space Res (Amst) **8**: 38-51.
33. Piggott, JJ, et al. (2015). "Reconceptualizing synergism and antagonism among multiple stressors." Ecology and Evolution: **5**(7): 1538–1547.
34. Piotrowski, I, et al. (2017). "Carcinogenesis Induced by Low-dose Radiation." Radiol Oncol **51**(4): 369-377.
35. Shuryak, I (2017). "Quantitative modeling of responses to chronic ionizing radiation exposure using targeted and non-targeted effects." PLoS One **12**(4): e0176476.
36. Siranart, N, et al. (2016). "Mixed Beam Murine Harderian Gland Tumorigenesis: Predicted Dose-Effect Relationships if neither Synergism nor Antagonism Occurs." Radiat Res **186**(6): 577-591.
37. Tang, J, et al. (2015). "What is synergy? The Saariselkä agreement revisited." Frontiers in Pharmacology **6**: 181.
38. Zaider, M, et al. (1980). "The synergistic effects of different radiations." Radiat Res **83**(3): 732-739.